Membrane Potential-Dependent Inactivation of Voltage-Gated Ion Channels in α-Cells Inhibits Glucagon Secretion From Human Islets

Reshma Ramracheya,[1] Caroline Ward,[1] Makoto Shigeto,[1] Jonathan N. Walker,[1,2] Stefan Amisten,[1] Quan Zhang,[1] Paul R. Johnson,[2,3] Patrik Rorsman,[1,2] and Matthias Braun[1]

OBJECTIVE—To document the properties of the voltage-gated ion channels in human pancreatic α-cells and their role in glucagon release.

RESEARCH DESIGN AND METHODS—Glucagon release was measured from intact islets. $[Ca^{2+}]_i$ was recorded in cells showing spontaneous activity at 1 mmol/l glucose. Membrane currents and potential were measured by whole-cell patch-clamping in isolated α-cells identified by immunocytochemistry.

RESULTS—Glucose inhibited glucagon secretion from human islets; maximal inhibition was observed at 6 mmol/l glucose. Glucagon secretion at 1 mmol/l glucose was inhibited by insulin but not by $ZnCl_2$. Glucose remained inhibitory in the presence of $ZnCl_2$ and after blockade of type-2 somatostatin receptors. Human α-cells are electrically active at 1 mmol/l glucose. Inhibition of K_{ATP}-channels with tolbutamide depolarized α-cells by 10 mV and reduced the action potential amplitude. Human α-cells contain heteropodatoxin-sensitive A-type K^+-channels, stromatoxin-sensitive delayed rectifying K^+-channels, tetrodotoxin-sensitive Na^+-currents, and low-threshold T-type, isradipine-sensitive L-type, and ω-agatoxin-sensitive P/Q-type Ca^{2+}-channels. Glucagon secretion at 1 mmol/l glucose was inhibited by 40–70% by tetrodotoxin, heteropodatoxin-2, stromatoxin, ω-agatoxin, and isradipine. The $[Ca^{2+}]_i$ oscillations depend principally on Ca^{2+}-influx via L-type Ca^{2+}-channels. Capacitance measurements revealed a rapid (<50 ms) component of exocytosis. Exocytosis was negligible at voltages below −20 mV and peaked at 0 mV. Blocking P/Q-type Ca^{2+}-currents abolished depolarization-evoked exocytosis.

CONCLUSIONS—Human α-cells are electrically excitable, and blockade of any ion channel involved in action potential depolarization or repolarization results in inhibition of glucagon secretion. We propose that voltage-dependent inactivation of these channels underlies the inhibition of glucagon secretion by tolbutamide and glucose. ***Diabetes*** **59:2198–2208, 2010**

From the [1]Oxford Centre for Diabetes Endocrinology and Metabolism, University of Oxford, Churchill Hospital, Oxford, U.K.; the [2]NIHR Oxford Biomedical Research Centre, Oxford, U.K.; and the [3]Nuffield Department of Surgery, John Radcliffe Hospital, Oxford, U.K.

Corresponding author: Matthias Braun, matthias.braun@drl.ox.ac.uk.

Received 9 October 2009 and accepted 8 June 2010. Published ahead of print at http://diabetes.diabetesjournals.org on 14 June 2010. DOI: 10.2337/db09-1505.

Glucagon is the principal hyperglycemic hormone (1,2). It is secreted from the pancreatic α-cells in response to a fall in plasma glucose levels, β-adrenergic stimulation, lipids, and amino acids (3–5). Glucagon secretion from α-cells is regulated by paracrine (3), neuronal (6), and intrinsic mechanisms (7). Diabetes involves both impaired insulin and glucagon secretion (8). Thus, hyperglucagonemia is thought to contribute to elevated blood glucose levels, and the impaired glucagon response to hypoglycemia represents a limiting factor for insulin treatment in both type 1 and type 2 diabetes (9,10).

Ion channels and electrical activity play a key role in the regulation of glucagon secretion. The properties of rodent α-cells have been characterized in some detail (5,11–13). Rodent α-cells are electrically excitable and electrically active in the absence of glucose. Action potential firing depends on the opening of voltage-activated L- and N-type Ca^{2+}-channels, tetrodotoxin (TTX)-sensitive Na^+-channels, and A-type K^+-channels (14).

The α-cells make up ~35% of the cell population in human islets (15,16). Here, we have characterized the electrophysiological properties of isolated human α-cells and correlated our findings to changes in glucagon secretion from intact human islets. Our data indicate that glucagon secretion depends on a complex interplay among a number of depolarizing and repolarizing membrane currents.

RESEARCH DESIGN AND METHODS

Islet isolation. Human pancreases were obtained with ethical approval and clinical consent from nondiabetic donors. Islets were isolated in the Diabetes Research & Wellness Foundation Human Islet Isolation Facility by collagenase digestion (Serva, Heidelberg, Germany), using modified versions of published procedures (17,18).

Glucagon secretion assay. Islets were cultured overnight in CMRL medium containing 5.5 mmol/l glucose and 2 mmol/l L-glutamine. Batches of 10–20 size-matched islets (in triplicates) were preincubated in Krebs-Ringer buffer (KRB) containing 2 mg/ml BSA and 1 mmol/l glucose for 1 h at 37°C, followed by a 1-h test incubation in KRB supplemented with glucose and ion channel blockers as indicated. The glucagon content of the supernatant was determined by radioimmunoassay (Millipore U.K. Ltd., Livingston, U.K.). Insulin and somatostatin were determined as described previously (19,20).

Electrophysiology. Freshly isolated islets were dispersed into single cells by trypsin digestion and plated onto plastic Petri dishes. The cells were cultured in RPMI medium containing 10 mmol/l glucose prior to the experiments. Patch-clamp experiments were performed by whole-cell measurements at ~32°C as previously described (19).

The extracellular solution for membrane potential measurements contained (in mM) 140 NaCl, 3.6 KCl, 0.5 $MgSO_4$, 1.5 $CaCl_2$, 10 HEPES, 0.5 NaH_2PO_4, 5 $NaHCO_3$ (pH adjusted to 7.4 with NaOH), and glucose as indicated. The extracellular solution for K^+-current measurements con-

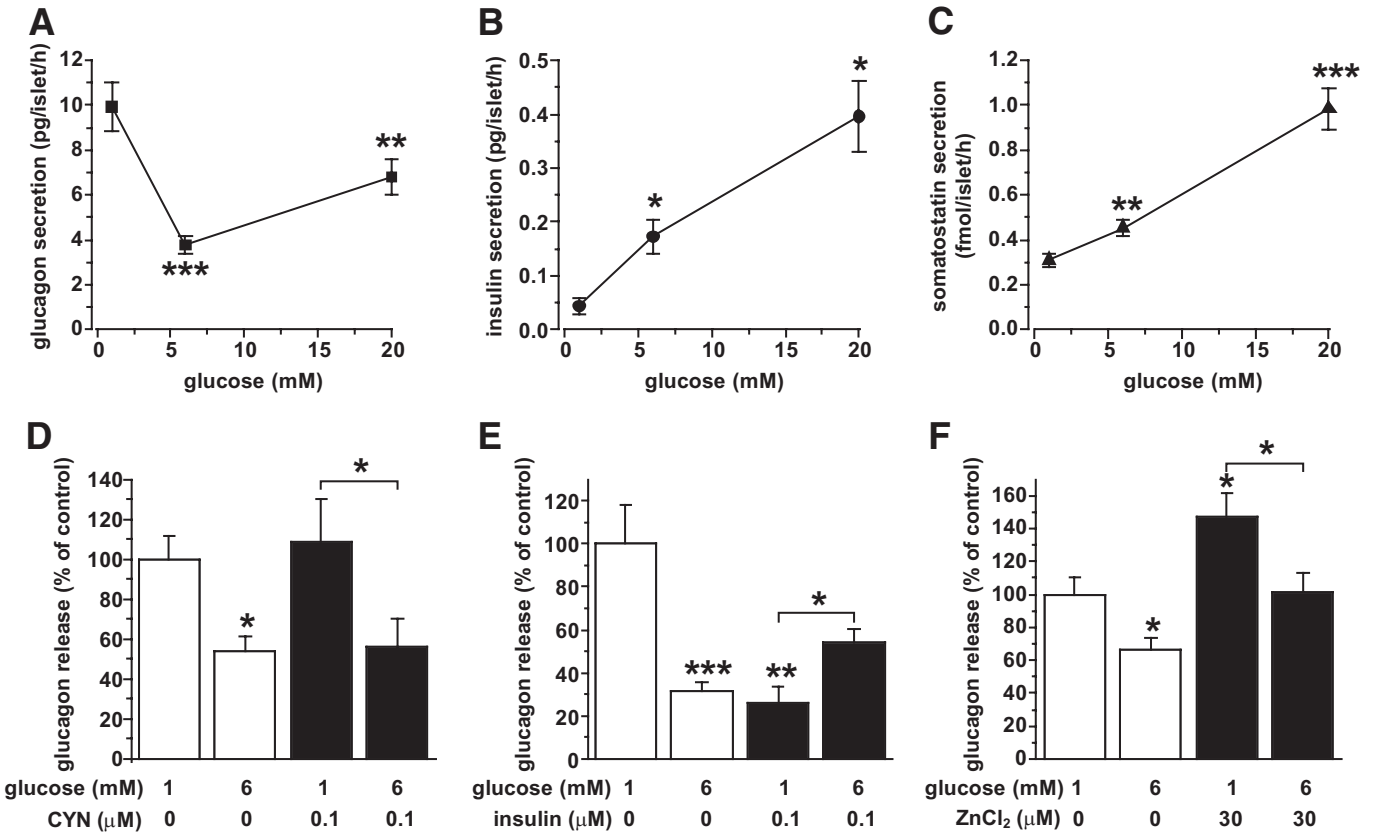

FIG. 1. Glucose dependence of glucagon secretion and effect of paracrine modulators. *A–C*: Secretion of glucagon (*A*), insulin (*B*), and somatostatin (*C*) measured at 1, 6, and 20 mmol/l glucose. Data are from 50 donors (glucagon) or 33 donors (insulin and somatostatin). **P* < 0.05, ***P* < 0.01, ****P* < 0.001 versus the previous lower glucose concentration. Glucagon secretion was significantly lower at 20 mmol/l compared with 1 mmol/l glucose (*P* < 0.05). *D*: Glucagon secretion measured at 1 and 6 mmol/l glucose under control conditions and in the presence of 100 nmol/l of CYN-154806 (CYN). 100% = 3.4 ± 0.4 pg glucagon/islet/h. *E*: As in *D* but in the absence and presence of 100 nmol/l insulin. 100% = 4.9 ± 0.9 pg glucagon/islet/h. *F*: As in *D* but in the absence and presence of 30 μmol/l $ZnCl_2$. 100% = 3.8 ± 0.5 pg glucagon/islet/h. *D–F*: **P* < 0.05, ***P* < 0.01, ****P* < 0.001 versus 1 mmol/l glucose (control) or as indicated by brackets.

tained (mM) 138 NaCl, 5.6 KCl, 2.6 $CaCl_2$, 1.2 $MgCl_2$, 5 HEPES, and 5 glucose (pH 7.4, with NaOH). For all other experiments, 20 mmol/l TEACl was added and NaCl was reduced correspondingly. Na^+- or Ca^{2+}-currents were recorded in the presence of 1 mmol/l $CoCl_2$ or 0.1 μg/ml TTX, respectively. The intracellular solution for recording voltage-gated K^+-currents was composed of (mM) 120 KCl, 1 $MgCl_2$, 10 EGTA, 1 $CaCl_2$, 10 HEPES, and 3 MgATP (pH 7.2, with KOH). To measure voltage-gated Na^+- or Ca^{2+}-currents, KCl was replaced equimolarly by CsCl. In capacitance measurements, the pipette solution was composed of (mM) 125 Cs-glutamate, 10 CsCl, 10 NaCl, 1 $MgCl_2$, 5 HEPES, 0.05 EGTA, 3 MgATP, and 0.1 cAMP (pH 7.15 with CsOH).

Membrane potential recordings were made using the perforated-patch whole-cell configuration. The intracellular solution contained (mM) 76 K_2SO_4, 10 KCl, 10 NaCl, 1 $MgCl_2$, 5 HEPES (pH 7.35 with KOH), and 0.24 mg/ml amphotericin B (21).

Immunocytochemistry. Immunocytochemical identification of patch-clamped cells was performed as described previously (20,22).

$[Ca^{2+}]_i$ measurements. Intact islets were loaded with the Ca^{2+}-indicator fluo-4 AM (2.5 μmol/l; Invitrogen, Carlsbad, CA) in CMRL medium for 1–8 h at room temperature. The islets were immobilized in the recording chamber using a wide-bore holding pipette and continuously perifused with KRB containing 1 mmol/l glucose. The bath temperature was kept at 37°C. Laser scanning confocal microscopy was performed using an LSM 510 META laser scanning module (Zeiss) mounted on an Axioskop 2FS microscope. Images were acquired at 2.5-s intervals and analyzed using Zeiss LSM 510 software. Increases in $[Ca^{2+}]_i$ are displayed as upward deflections.

Data analysis. All data are expressed as means ± SEM. Glucagon secretion data have (except for Fig. 1) been normalized to secretion measured at 1 mmol/l glucose in the absence of blockers. Statistical significance was evaluated using Student *t* test. All hormone secretion experiments were repeated using islets from at least three donors.

RESULTS

Effects of glucose on pancreatic hormone release in human islets. Glucagon secretion was measured from intact human islets exposed to 1, 6, and 20 mmol/l glucose. Increasing the glucose concentration inhibited glucagon secretion; maximal inhibition (−62%) was observed at 6 mmol/l glucose (Fig. 1*A*). Increasing glucose from 6 to 20 mmol/l was associated with reduced inhibition, as previously observed in mouse islets (23). The effects of glucose on glucagon secretion were compared with those on insulin and somatostatin secretion. At 6 mmol/l glucose, stimulation of insulin and somatostatin secretion was only 37 and 21%, respectively, of that produced by 20 mmol/l glucose (Fig. 1*B* and *C*).

The somatostatin-receptor subtype 2 specific antagonist CYN-154806 (0.1 μmol/l) did not affect the ability of 6 mmol/l glucose to inhibit glucagon secretion (Fig. 1*D*). It was ascertained that the CYN-154806 antagonized the effects of somatostatin on α-cell membrane potential and $[Ca^{2+}]_i$ (supplementary Fig. S1, available in an online appendix at http://diabetes.diabetesjournals.org/cgi/content/full/db09-1505/DC1).

When applied at 1 mmol/l glucose, insulin (100 nmol/l) inhibited glucagon secretion by 74%, similar to the inhibition produced by 6 mmol/l glucose. Addition of insulin to islets exposed to 6 mmol/l glucose stimulated glucagon secretion (Fig. 1*E*). $ZnCl_2$ (30 μmol/l) increased glucagon

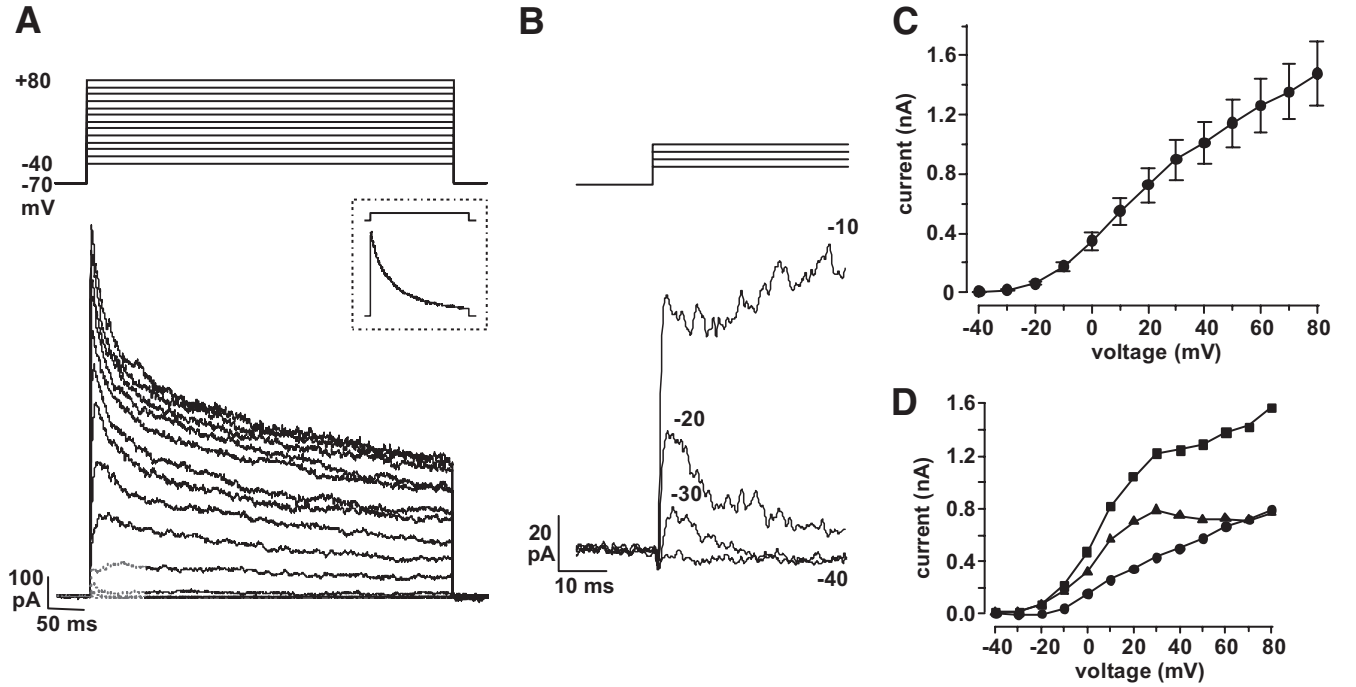

FIG. 2. Analysis of voltage-gated K^+-currents. *A*: Family of voltage-activated K^+-currents (lower) evoked by depolarizing pulses from −70 mV to membrane potentials between −40 and +80 mV. Inset shows inactivation of current during a 15-s depolarization from −70 to +20 mV. *B*: As in *A* but showing the initial part of the current responses during pulses to −40, −30, −20, and −10 mV on an expanded time base (sections highlighted in gray in *A*). *C*: *I–V* relationship for voltage-gated K^+-current (n = 8). *D*: Example of a cell showing a clear shoulder on the *I–V* at voltages between +30 and +50 mV. Data are shown for the peak current (*squares*), the sustained current measured at the end of the 500-ms pulse (*circles*), and the difference (*triangles*).

secretion at 1 and 6 mmol/l glucose by ~50% but did not affect the suppression of glucagon release by glucose (Fig. 1*F*). Neither insulin nor $ZnCl_2$ affected the spontaneous $[Ca^{2+}]_i$-oscillations observed at 1 mmol/l glucose (supplementary Fig. S2, available in an online appendix).

Voltage-gated K^+-currents. All electrophysiological recordings were conducted in individual human α-cells subsequently identified by immunocytochemistry. The α-cells had a membrane capacitance of 3.3 ± 0.1 pF (n = 197).

Voltage-gated membrane currents were recorded using the standard whole-cell configuration. Outward voltage-activated K^+-currents became detectable during membrane depolarizations from −70 to −30 mV and above (Fig. 2*A* and *B*). At −30 mV, the K^+-current inactivated completely within ~20 ms, whereas a sustained component was observed during depolarizations to −20 mV and above (Fig. 2*B*). The peak amplitude recorded during depolarizations to 0 mV averaged 349 ± 61 pA (n = 8). The inactivation of the current could be described as the sum of two exponentials with time constants (at +30 mV) of 18 ± 2 and 567 ± 147 ms (n = 7). The sustained current inactivated by >90% over 15 s (Fig. 2*A*, inset).

Figure 2*C* shows the *I–V* relationship recorded from eight cells. In three of the eight cells, a prominent shoulder on the *I–V* was seen at membrane potentials between +30 and +50 mV. Figure 2*D* shows the peak current, the sustained current measured at the end of the 500 ms depolarization, and the difference between the peak and the sustained currents in one of these cells. The difference current peaked at +30 mV. Similar current responses are seen in human β-cells (20) and reflect activation of large-conductance Ca^{2+}-activated K^+-channels (BK-channels; compare with ref [24]).

The broad-spectrum K^+-channel blocker tetraethylammonium (TEA) (10 mmol/l) inhibited 74 ± 2% (n = 6; P < 0.01) of the peak current and 87 ± 4% (n = 6; P < 0.01) of the sustained current evoked by depolarizations to +30 mV (Fig. 3*A*). The TEA-resistant transient component was completely blocked by 4-aminopyridine (5 mmol/l, n = 4; Fig. 2*A*). These pharmacological properties are those expected for A-type K^+-currents (A-current) (25). The selective K_V2.1/2.2 channel blocker stromatoxin (26) reduced the sustained current by 88 ± 5% (P < 0.01, n = 4) but decreased the peak current by only 33 ± 15% (P = 0.05; Fig. 3*B*). During depolarizations to 0 mV, the TEA- and stromatoxin-resistant A-current underwent rapid activation and inactivation. In seven different cells, the time constants of activation (τ_n) and inactivation (τ_h) averaged 0.26 ± 0.06 and 12 ± 3 ms, respectively (τ_n and τ_h were estimated assuming n^4h kinetics). τ_n decreased with increasing voltages (reflecting more rapid activation), whereas no clear voltage dependence of τ_h was observed (not shown). The A-current was sensitive to the selective K_V4.x-antagonist heteropodatoxin-2 (27) (Fig. 3*C*; n = 3).

Steady-state inactivation of voltage-gated K^+-currents was examined using two-pulse protocols in which conditioning pulses to between −90 and −20 mV preceded an activating test pulse (Figs. 3*D* and *E*). Both the A-type and the sustained K^+-current underwent voltage-dependent inactivation that could be described by Boltzmann functions (Fig. 3*F*). Half-maximal inactivation (V_h) of the A-current (studied in the presence of TEA) was observed at −49 ± 2 mV; the slope factor (n_h) averaged −4.8 ± 0.4 mV (n = 7; Fig. 3*D* and *F*). The delayed-rectifier current (ignoring the initial 50 ms to avoid contamination by the A-current) inactivated at more positive potentials with V_h

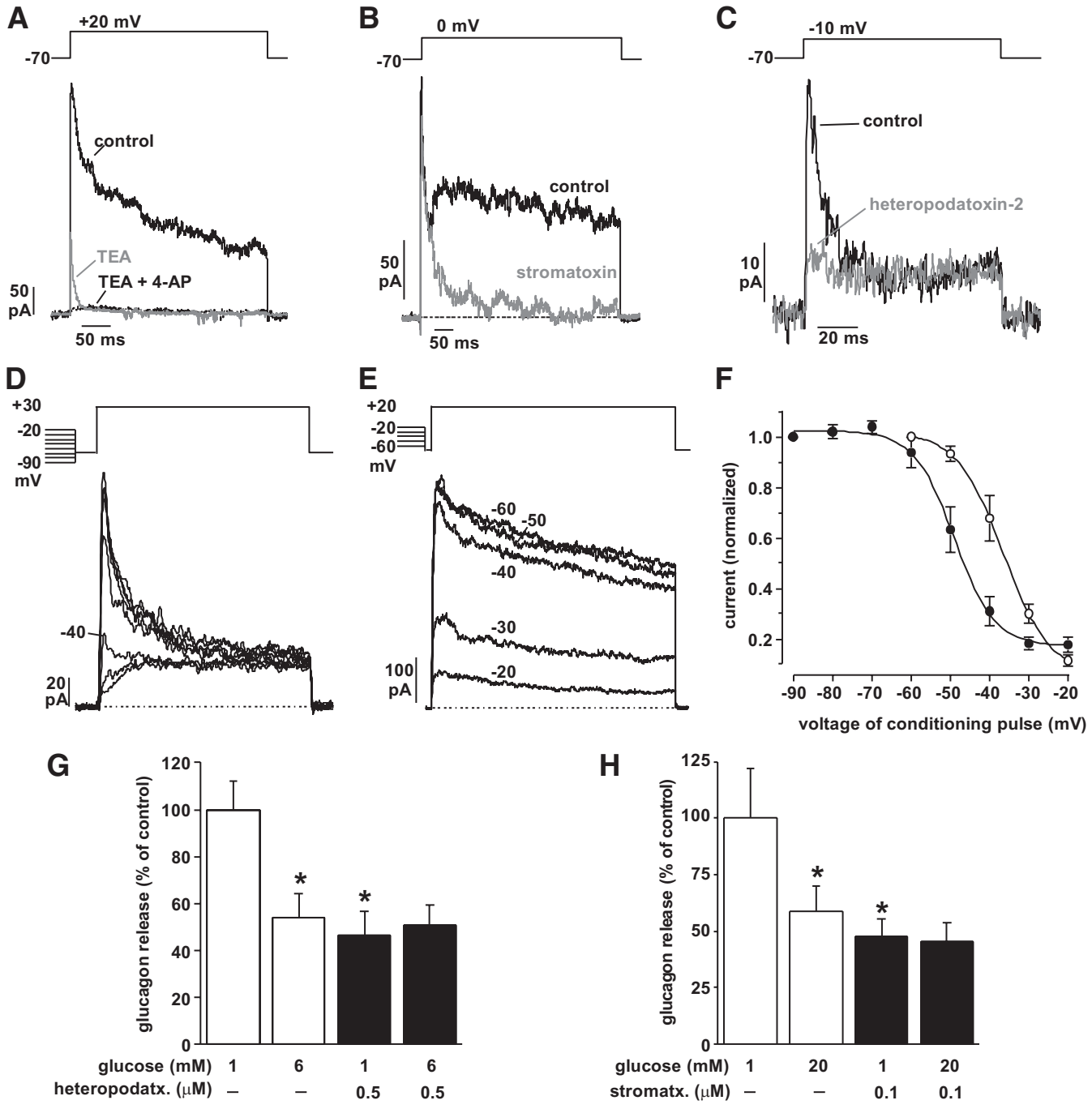

FIG. 3. Pharmacological characterization of voltage-gated K^+-currents. *A*: Current responses recorded during depolarizations to +20 mV under control conditions, after addition of 10 mmol/l TEA (gray trace) and after addition of 5 mmol/l 4-aminopyridine in the continued presence of TEA ($n = 4$). *B*: As in *A* but pulse went to zero and currents were recorded in the absence and presence of stromatoxin (100 nmol/l, $n = 4$). *C*: As in *A* but pulse went to −10 mV and currents were recorded in the presence of 10 mmol/l TEA before and after application of heteropodatoxin-2 (0.5 μmol/l). *D*: Steady-state inactivation of the A-current analyzed by a two-pulse protocol consisting of a 200-ms conditioning pulse to membrane potentials between −90 and −20 mV followed by a 100-ms test pulse to +30 mV after an interval of 10 ms. Experiments were performed using the perforated-patch technique in the presence of TEA. *E*: Steady-state inactivation of the delayed-rectifying K^+-current was measured by applying 15-s conditioning pulses to membrane potentials between −60 and −20 mV followed by a 500-ms test pulse to +20 mV (interval 10 ms). *F*: Voltage dependence of inactivation of A-current (closed circles) and delayed-rectifier current (open circles). The responses after conditioning pulses to −90 and −60 mV, respectively, were taken as unity, and data are presented as a fraction of the maximal current displayed against the voltage during the conditioning pulse. A Boltzmann function has been fit to the data points ($n = 5$–7). *G*: Glucagon secretion measured in the absence (open bars) and presence (filled bars) of 0.5 μmol/l heteropodatoxin-2 at 1 or 6 mmol/l glucose. *$P < 0.01$ versus 1 mmol/l glucose alone. 100% = 6.5 ± 0.8 pg/islet/h ($n = 12$; 4 donors). *H*: Effects of 100 nmol/l stromatoxin on glucagon secretion at 1 or 20 mmol/l glucose. *$P < 0.05$ versus 1 mmol/l glucose. 100% = 7.5 ± 1.5 pg/islet/h ($n = 9$; 3 donors).

and n_h amounting to −37 ± 2 and 5 ± 1 mV, respectively ($n = 5$; Fig. 3*E* and *F*).

The recovery of A-current from inactivation was measured by application of two 50-ms test pulses to +30 mV separated by a conditioning pulse to −70 mV of increasing duration. The current recovered rapidly with a time constant of 45 ± 7 ms ($n = 4$; supplementary Fig. 3*A* and *B*, available in an online appendix). This behavior is charac-

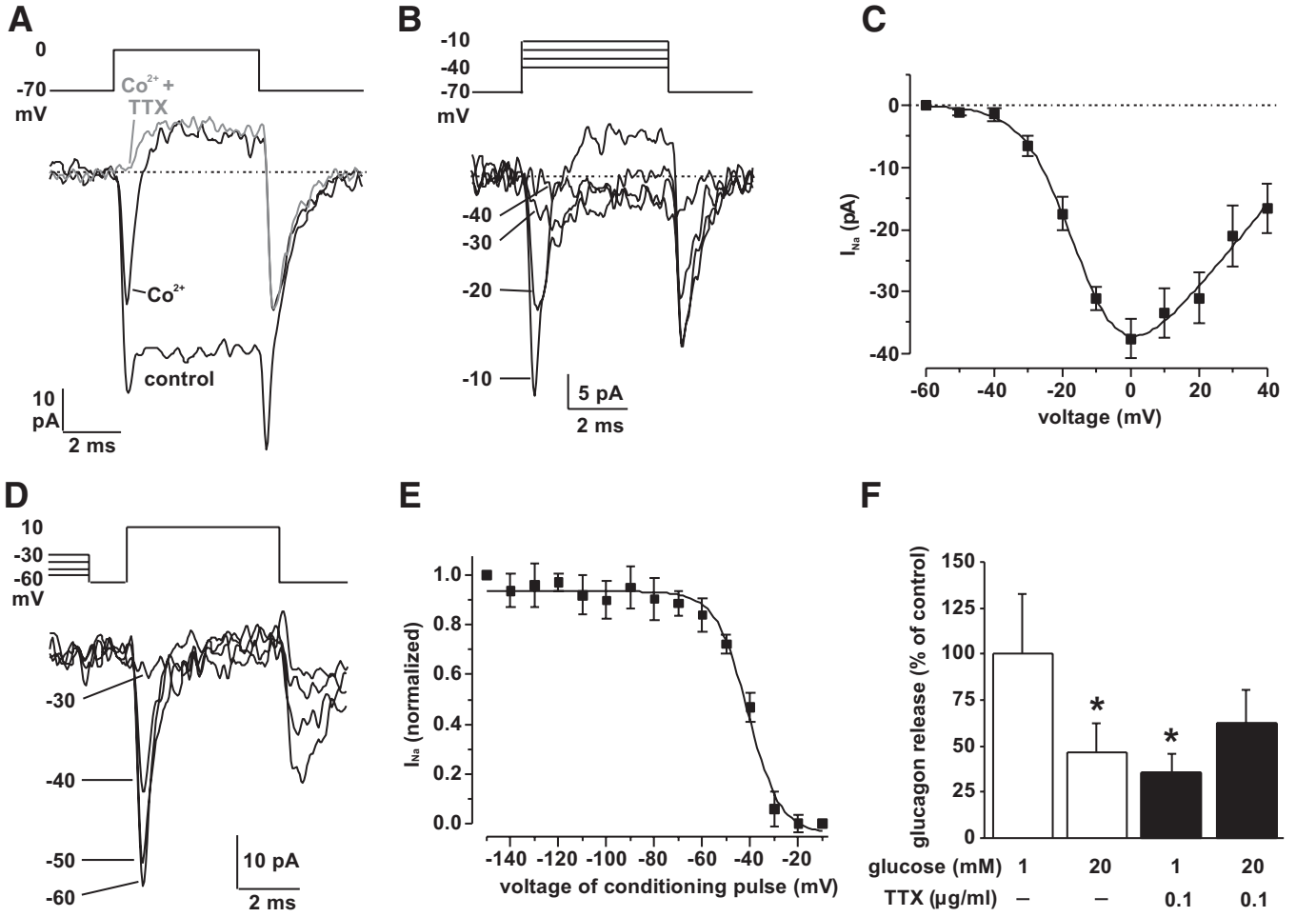

FIG. 4. Voltage-gated TTX-sensitive Na^+-channels. Experiments were performed in the presence of TEA (10 mmol/l) in the extracellular solution and after replacing K^+ with Cs^+ in the pipette solution. *A*: Currents recorded under control conditions, after addition of 1 mmol/l Co^{2+} and after addition of TTX (0.1 μg/ml) in the continued presence of Co^{2+}. *B*: Voltage dependence of Na^+-currents. The responses recorded in the presence of Co^{2+} during depolarizations to −40, −30, −20, and −10 mV are shown. *C*: *I–V* relationship for Na^+-currents (n = 5). *D*: Inactivation of Na^+-current. A test pulse to +10 mV was preceded by 50-ms conditioning pulses to membrane potentials between −150 and 0 mV (−60 to −30 shown). Currents were recorded in the presence of Co^{2+}. *E*: Inactivation curve. The response after a conditioning pulse to −150 mV was taken as unity (n = 6). A Boltzmann function fit to the mean data has been superimposed. *F*: Glucagon secretion measured in the absence (open bars) and presence (filled bars) of TTX (0.1 μg/ml) at 1 or 20 mmol/l glucose as indicated. 100% = 12.2 ± 3.8 pg/islet/h (n = 15; 4 donors). *P < 0.05 versus 1 mmol/l glucose alone.

teristic of K_V4.x mediated A-currents (28). The delayed-rectifier K^+-current recovered from inactivation (induced by a 15-s depolarization to −20 mV) with a τ of 2.9 ± 0.7 s (n = 4, supplementary Fig. 3*C*).

Glucagon secretion at 1 mmol/l glucose was inhibited by heteropodatoxin-2 (Fig. 3*G*) and stromatoxin (Fig. 3*H*). The inhibitory effect of the K^+-channel blockers was comparable to that produced by 6 or 20 mmol/l glucose. Glucose did not exert any additional inhibitory effect in the presence of either blocker. Blockade of A-currents with 4-aminopyridine (5 mmol/l) inhibited glucagon secretion as strongly as heteropodatoxin-2 (not shown).

Voltage-gated Na^+-currents. Voltage-gated inward currents were studied using Cs^{2+}-containing pipette solution and TEA-containing bath solution to block K^+-currents. Figure 4*A* shows membrane currents elicited by 5-ms depolarizations from −70 to 0 mV. Under control conditions, the response consisted of an initial transient component followed by a sustained current. The sustained current was inhibited by the broad-spectrum Ca^{2+}-channel blocker Co^{2+} (1 mmol/l). In the presence of Co^{2+}, a rapidly activating and inactivating current was observed that was inhibited by the Na^+-channel blocker TTX.

The Na^+-current became detectable during depolarizations to −30 mV and above (Fig. 4*B*). The *I–V* relationship exhibited a U-shaped voltage dependence with a maximal amplitude of −38 ± 3 pA at 0 mV (n = 5; Fig. 4*C*). Both the activation and deactivation of the Na^+-current became faster with increasing voltages (not shown).

The Na^+-current in human α-cells undergoes voltage-dependent inactivation (Fig. 4*D*). The steady-state inactivation properties are summarized in Fig. 4*E*; V_h and n_h averaged −40 ± 2 and 5 ± 1 mV (n = 6), respectively.

The effect of the Na^+-channel blocker TTX on glucagon secretion from intact human islets is shown in Fig. 4*F*. The inclusion of TTX in the extracellular medium reduced glucagon secretion as strongly as 20 mmol/l glucose, and glucose lacked further inhibitory action in the presence of the blocker.

Voltage-gated Ca^{2+}-currents. Voltage-gated Ca^{2+}-currents (responsible for the sustained current component in Fig. 4*A*) were examined in the presence of the Na^+-channel blocker TTX. Figure 5*A* shows a family of voltage-clamp currents elicited by membrane depolarization from −70 mV to voltages between −60 and 0 mV. The voltage dependence of the α-cell Ca^{2+}-current is shown in Fig. 5*B*.

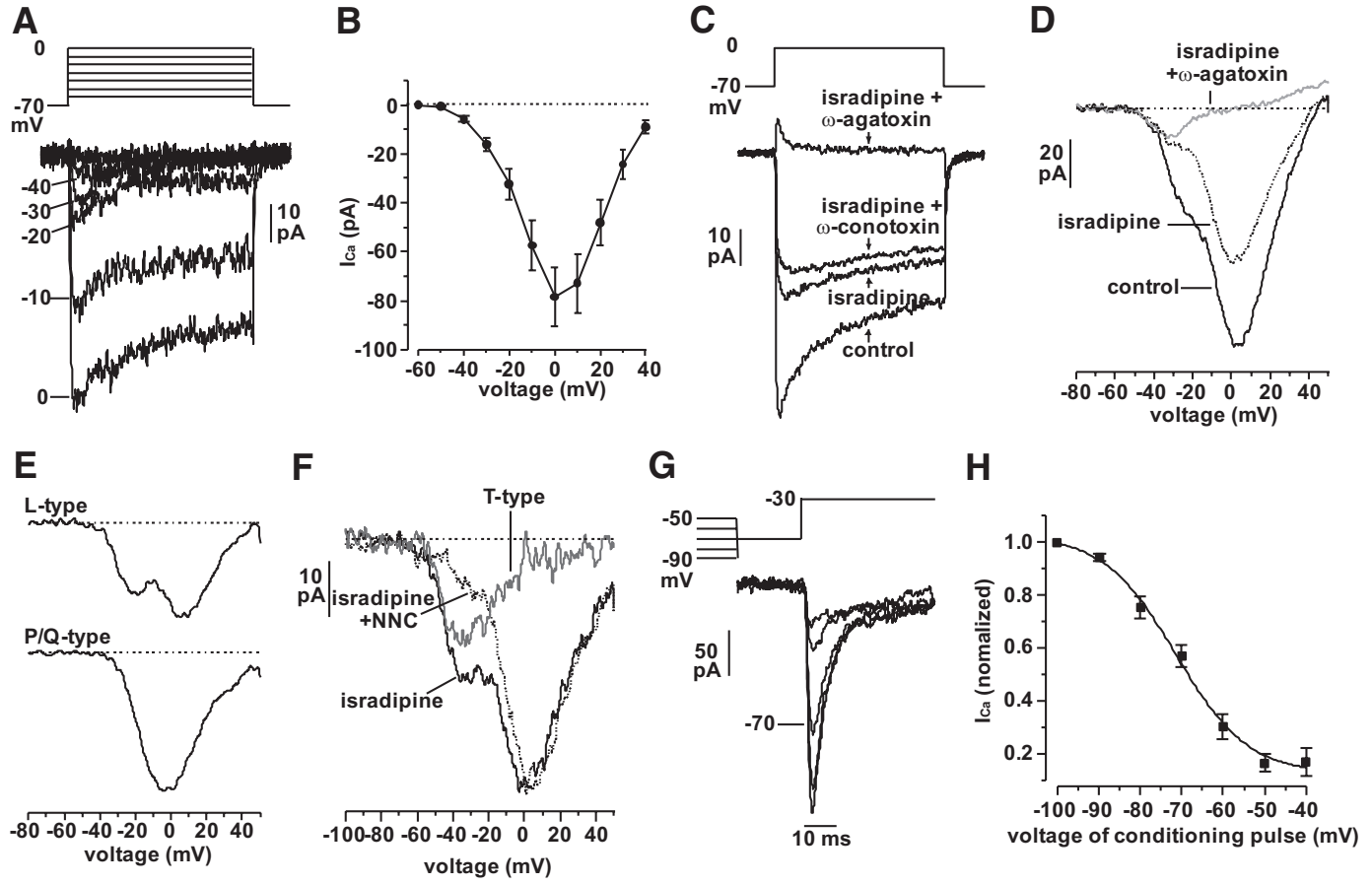

FIG. 5. Voltage-gated Ca^{2+}-currents. Experiments were performed with TEA-containing extracellular and Cs^{+}-containing pipette solution. *A*: Family of voltage-gated Ca^{2+}-currents recorded in the presence of TTX during 100-ms depolarizations to between −60 and 0 mV as indicated. *B*: Current voltage relationship of whole-cell Ca^{2+}-currents (n = 14). *C*: Ca^{2+}-current recorded under control conditions and after addition of 10 μmol/l isradipine and ω-conotoxin (100 nmol/l) and ω-agatoxin (200 nmol/l) in the continued presence of isradipine as indicated. *D*: Ca^{2+}-currents elicited by voltage ramps (speed, 3 V/s) under control conditions and after addition of isradipine and ω-agatoxin in the continued presence of isradipine (n = 7, 7, 4 under control conditions, in the presence of isradipine, and after addition of ω-agatoxin, respectively). *E*: Isradipine- (top) and ω-agatoxin-sensitive components (lower) from *D*. *F*: Ca^{2+}-currents elicited by voltage ramps in the presence of isradipine alone (10 μmol/l) and after addition of NNC 55-0396 (3 μmol/l) in the continued presence of isradipine. The difference current (T-type; gray) is also shown. *G*: Inactivation of the T-type Ca^{2+}-current. A test pulse to −30 mV was preceded by 500-ms conditioning pulses to membrane potentials between −90 and −50 mV (in the presence of 10 μmol/l isradipine). *H*: Voltage-dependent inactivation of T-type Ca^{2+}-current. The current elicited after a conditioning pulse to −100 mV was taken as unity. A Boltzmann fit has been superimposed on the data points (n = 6, experiments performed in the presence of isradipine).

The current became detectable at voltages above −50 mV and peaked at 0 mV, where the amplitude averaged −67 ± 7 pA (n = 19).

The pharmacological properties of the Ca^{2+}-current are shown in Fig. 5*C*. The Ca^{2+}-currents in human α-cells are sensitive to the L-type Ca^{2+}-channel blocker isradipine and the P/Q-type Ca^{2+}-channel antagonist ω-agatoxin IVA. The isradipine- and ω-agatoxin-sensitive currents accounted for 21 ± 4% ($P < 0.01$; n = 9) and 70 ± 6% ($P < 0.01$; n = 5) of the integrated Ca^{2+}-current (Q_{Ca}), respectively. In addition, we observed a small current component blocked by the N-type channel blocker ω-conotoxin GVIA (11 ± 3% reduction of Q_{Ca}; $P < 0.01$; n = 13).

Voltage ramps between −80 and +50 mV were used to determine the voltage dependence of the different Ca^{2+}-current components (Fig. 5*D*). Under control conditions, inward currents became detectable above −50 mV and the current amplitude then showed a triphasic dependence on membrane potential: a shoulder between −40 and −20 mV, a secondary acceleration between −20 and 0 mV, and a subsequent decline at more positive voltages (reflecting the reduced electrochemical driving force). Also shown in Fig. 5*D* are the responses recorded after addition of isradipine alone and the combination of isradipine and ω-agatoxin, respectively. Figure 5*E* shows the net isradipine- (L-type; upper panel) and ω-agatoxin-sensitive (P/Q-type; lower panel) Ca^{2+}-currents. Whereas the activation of the P/Q-type current was monophasic, that of the L-type current was biphasic. The latter feature might reflect the expression of two L-type Ca^{2+}-channel isoforms in human islets (α1C and α1D; [20]). It is evident from Fig. 5*D* that a small current component activating at negative voltages (below −50 mV) is resistant to all these Ca^{2+}-channel blockers. This current reflects opening of low-threshold T-type Ca^{2+}-channels. Figure 5*F* shows current responses elicited by ramps in the presence of isradipine alone and in the combined presence of the T-type Ca^{2+}-channel antagonist NNC 55-0396. The gray trace in Fig. 5*F* represents the net NNC 55-0396-sensitive T-type Ca^{2+}-current. The low-threshold T-type current was seen in 10 of 14 cells and gave rise to a rapidly inactivating current during depolarization to −30 mV (Fig. 5*G*). The T-type current undergoes voltage-dependent inactivation with values for V_h and n_h of −71 ± 2 and 8 ± 1 mV, respectively (n = 6; Fig. 5*G* and *H*). The T-type Ca^{2+}-current was not observed during depolarizations to 0 mV (Fig. 5*C*) because it is obscured by

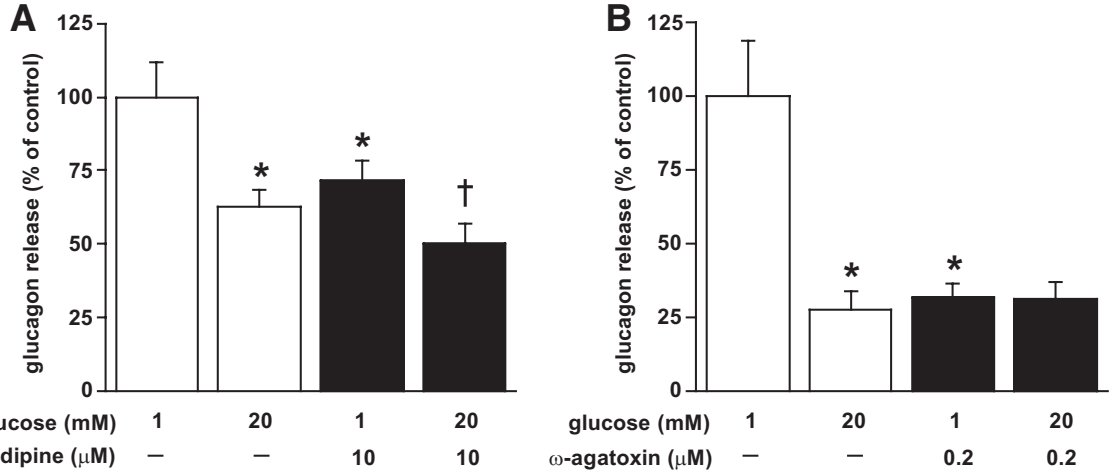

FIG. 6. Effects of Ca^{2+}-channel antagonists on glucagon secretion. *A*: Glucagon secretion measured in the absence (open bars) and presence (filled bars) of 10 μmol/l isradipine. *$P < 0.01$ versus 1 mmol/l glucose alone, †$P < 0.05$ versus 1 mmol/l glucose and 10 μmol/l isradipine. 100% = 10.5 ± 0.6 pg/islet/h ($n = 9$; 3 donors). *B*: Same as in *A* but effects of 200 nmol/l ω-agatoxin were tested. *$P < 0.01$ versus 1 mmol/l glucose alone, 100% = 21.1 ± 3.7 pg/islet/h ($n = 9$; 3 donors).

a transient outward current that reflects efflux of Cs^+ via A-type K^+-channels (not shown).

The L-type Ca^{2+}-channel blocker isradipine inhibited glucagon secretion from human islets at 1 mmol/l glucose by 25% (Fig. 6*A*). Glucose retained an inhibitory action in the presence of isradipine ($P < 0.05$). Blocking the P/Q-type Ca^{2+}-channels exerted a stronger suppressor effect and was as inhibitory as 20 mmol/l glucose (Fig. 6*B*). Glucose did not diminish glucagon secretion when applied in the presence of ω-agatoxin. The T-type Ca^{2+}-channel blocker 55-0396 paradoxically increased secretion at 1 mmol/l glucose by 190 ± 30% ($n = 3$; $P < 0.05$) but did not affect the inhibitory action of 20 mmol/l glucose (65 ± 5%; $n = 3$; $P < 0.05$; not shown). The stimulation of glucagon secretion by the T-type Ca^{2+}-channel blocker cannot be attributed to inhibition of somatostatin or insulin secretion (19,20) and may therefore reflect an unspecific action of the compound.

Background membrane conductance, electrical activity, and $[Ca^{2+}]_i$. The background membrane conductance of α-cells was measured in the perforated-patch whole-cell configuration by applying 10 mV depolarizing pulses from −70 mV. The membrane conductance at 1 mmol/l glucose averaged 0.12 ± 0.01 nS ($n = 27$). It was not reduced by elevation of glucose to 6–10 mmol/l (0.12 ± 0.04 nS; $n = 13$) or after addition of 100 μmol/l tolbutamide (0.11 ± 0.04 nS, $n = 13$). However, diazoxide (100 μmol/l) increased the membrane conductance (from 0.14 ± 0.05 to 0.32 ± 0.12 nS; $P = 0.05$, $n = 7$).

Regenerative electrical activity was observed in 31 of 43 α-cells analyzed (Fig. 7*A*). Of these, 76% were continuously active, whereas the action potentials tended to be grouped in bursts in the remaining 24% of the cells. Action potentials were initiated from an average threshold potential of −42 ± 1 mV and peaked at 2 ± 1 mV ($n = 26$). The membrane potential of α-cells was unaffected by increasing the glucose concentration (−39 ± 5 mV at 1 mmol/l glucose and −37 ± 4 mV at 6–10 mmol/l, $n = 15$), but tolbutamide (100–400 μmol/l) depolarized the cells by ~10 mV, from −42 ± 3 to −32 ± 2 mV ($P < 0.001$, $n = 9$). This was associated with a reduction of action potential peak voltage from −5 ± 3 to −12 ± 2 mV ($P < 0.05$; Fig. 7*B*). Diazoxide (100 μmol/l) hyperpolarized the α-cell membrane potential by 19 ± 4 mV ($P < 0.05$, $n = 5$; not shown). For unknown reasons, regenerative electrical activity subsided rapidly in most cells and was replaced by small and irregular membrane potential oscillations. This precluded a detailed analysis of the effects of different ion channel blockers on α-cell electrical activity.

Many cells in intact human islets exposed to 1 mmol/l glucose exhibited spontaneous oscillations in cytosolic Ca^{2+}-concentration ($[Ca^{2+}]_i$). Of these cells, 71% responded with a large elevation of $[Ca^{2+}]_i$ when exposed to 5 μmol/l adrenaline (Fig. 7*C*). This feature is characteristic of α-cells in mouse islets (29). Experiments on isolated human islet cells revealed that 77% of the cells that responded to adrenaline with an elevation of $[Ca^{2+}]_i$ were α-cells (as determined by immunocytochemistry). Addition of 200 nmol/l ω-agatoxin had a small inhibitory effect on $[Ca^{2+}]_i$, whereas subsequent addition of 10 μmol/l isradipine was strongly inhibitory, an effect that could not be antagonized by BayK8644 in islets that had been exposed to ω-agatoxin (Fig. 7*D*). Application of isradipine to islets that had *not* been exposed to ω-agatoxin also reduced $[Ca^{2+}]_i$, but under these conditions, the effect was partially antagonized by BayK8644 (Fig. 7*E*). The experiments were concluded by depolarizing the cells with 70 mmol/l K^+. The amplitude of the response to high $[K^+]_o$ was much larger when the cells had not been exposed to ω-agatoxin ($P < 0.001$).

Exocytosis in human α-cells. High-resolution capacitance measurements were applied to examine the exocytotic properties of individual α-cells. The time course of exocytosis was monitored by applying progressively longer depolarizing pulses (20–500 ms) from −70 to 0 mV (Fig. 8*A*). The amplitude of the responses was typically fairly small and limited to 40 ± 5 fF ($n = 32$) for a 500-ms depolarization. However, pulses as short as 20 ms elicited good responses in ~50% of the cells. Figure 8*B* summarizes the relationship between the duration of the depolarizing command and the exocytotic response. The average responses tended to plateau within 50–100 ms with a secondary acceleration becoming apparent for pulse durations ≥200 ms.

The voltage dependence of exocytosis in α-cells is shown in Fig. 8*C*. Responses were small for depolarizations to membrane potentials more negative than −10 mV.

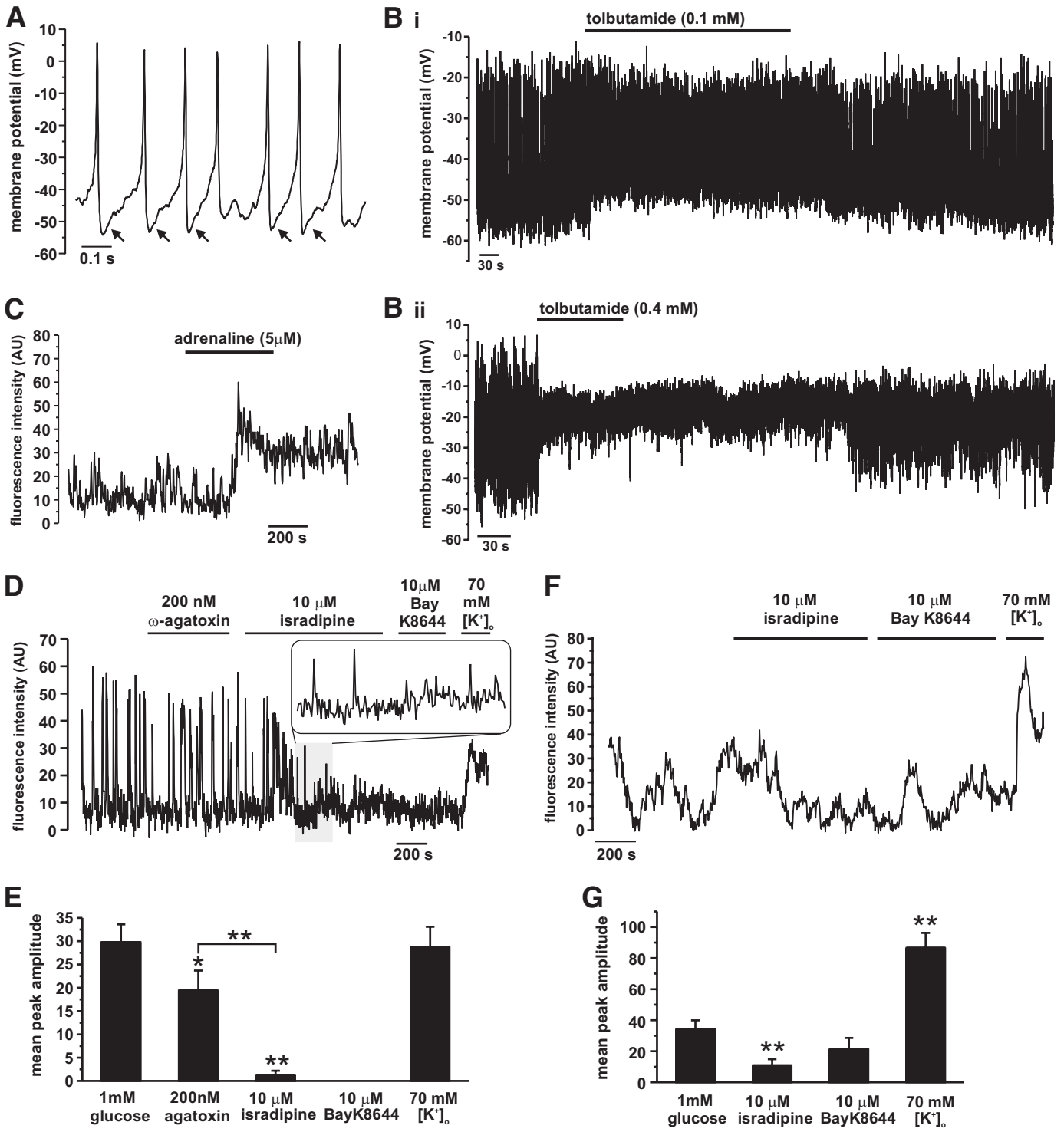

FIG. 7. Electrical activity and $[Ca^{2+}]_i$ oscillations. *A*: Membrane potential recording from an α-cell exposed to 1 mmol/l glucose. Note prominent after-hyperpolarizations after each action potential (arrows). *B*: Effect of tolbutamide on α-cell membrane potential in two representative cells. Note reduction of peak voltage. *C*: Spontaneous $[Ca^{2+}]_i$ oscillations in an α-cell within an intact islet exposed to 1 mmol/l glucose before and during addition of 5 μmol/l adrenaline. *D*: As in *C* but testing the effects of ω-agatoxin (200 nmol/l), isradipine (10 μmol/l), Bay K8644 (10 μmol/l), and K^+ (70 mmol/l) at 1 mmol/l glucose. The *inset* shows the segment of the recording highlighted in gray on an expanded timebase. *E*: Histogram summarizing the average amplitude of the $[Ca^{2+}]_i$ oscillations under the indicated experimental conditions (13 cells in four islets obtained from two donors; *$P < 0.01$, **$P < 0.001$ vs. 1 mmol/l glucose or as indicated by brackets). *F*: As in *D* but ω-agatoxin was not applied. *G*: Histogram summarizing results obtained as described in *F* from 14 cells in four islets from two donors ($P < 0.001$ vs. 1 mmol/l glucose).**

The maximum responses were observed during depolarizations to 0 mV.

As shown in Fig. 8*D*, exocytosis elicited by a 500-ms depolarization from −70 to 0 mV was inhibited by 97 ± 3% ($P < 0.05$; $n = 4$) by ω-agatoxin. Exocytosis was not affected by stromatoxin, heteropodatoxin-2, and TTX

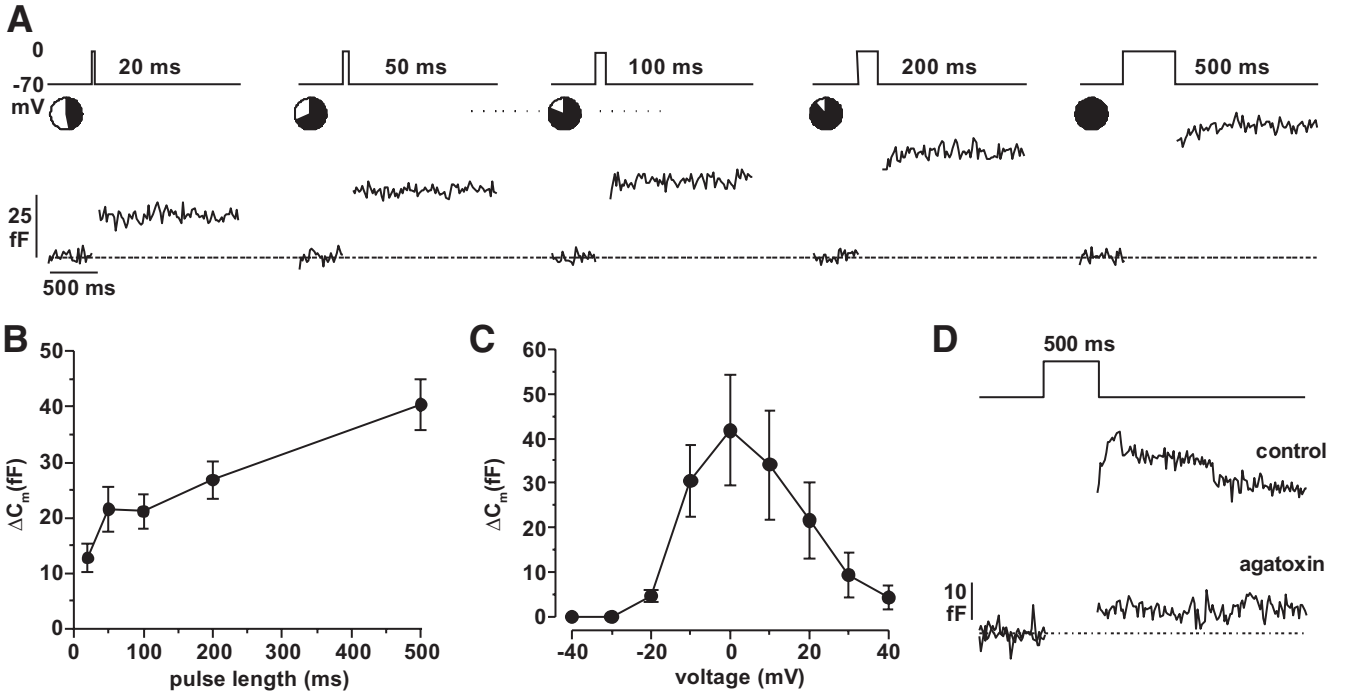

FIG. 8. Capacitance measurements of exocytosis. *A*: Increase in membrane capacitance evoked by 20–500-ms depolarizations from −70 to 0 mV. The circles above the capacitance traces indicate the percentage of responding cells (black part, $n = 23$). *B*: Relationship between pulse duration and exocytotic response (ΔC_m; $n = 23$). *C*: Change in cell capacitance (ΔC_m) evoked by 500-ms depolarizations from −70 mV to membrane potentials between −40 and +40 mV ($n = 8$). *D*: Change in cell capacitance evoked by 500-ms depolarization from −70 to 0 mV under control conditions and after addition of ω-agatoxin (200 nmol/l).

(~90% of control) but was strongly reduced (>75%) by 4-aminopyridine. Thus, the strong inhibitory effect of 4-aminopyridine on glucagon secretion may result from direct interference with α-cell exocytosis.

DISCUSSION

We have conducted the first electrophysiological characterization of the ion channels involved in human α-cell action potential firing and glucagon secretion. We demonstrate that human α-cells, like their rodent counterparts (13), are electrically active at low glucose concentrations and generate spontaneous oscillations in $[Ca^{2+}]_i$. The spontaneous $[Ca^{2+}]_i$ oscillations observed at 1 mmol/l glucose were reduced (but not abolished) by the L-type Ca^{2+}-channel blocker isradipine, an effect that could be antagonized by the L-type Ca^{2+}-channel agonist BayK8644. The isradipine-resistant $[Ca^{2+}]_i$ oscillations are likely to reflect Ca^{2+}-influx via P/Q-type and/or T-type Ca^{2+}-channels. In agreement with this interpretation, the $[Ca^{2+}]_i$-oscillations were completely suppressed when isradipine was applied to islets exposed to the P/Q-type Ca^{2+}-channel blocker ω-agatoxin. Collectively, these findings make clear that the $[Ca^{2+}]_i$ oscillations depend on influx of extracellular Ca^{2+}.

It is surprising that ω-agatoxin alone only had a minor effect on $[Ca^{2+}]_i$ although it strongly suppressed glucagon secretion and P/Q-type channels account for 70% of the whole-cell Ca^{2+}-currents. This indicates that these channels activate very briefly during the peak of the action potentials and therefore mediate only a fraction of the Ca^{2+}-entry during electrical activity. These observations suggest that P/Q-type Ca^{2+}-channels are tightly linked to the exocytosis of the glucagon granules. Indeed, the capacitance measurements revealed that depolarization-evoked exocytosis was completely dependent on Ca^{2+}-influx through P/Q-type Ca^{2+}-channels.

We addressed the potential roles of somatostatin and insulin as paracrine regulators of glucagon secretion. Blocking somatostatin-receptor subtype 2 (the subtype expressed in human α-cells; supplementary Fig. S1 and ref [30]) does not interfere with the ability of glucose to inhibit glucagon secretion. In accordance with previous in vivo observations in human (31) and isolated mouse islets (32), insulin inhibited glucagon secretion from human islets exposed to 1 mmol/l glucose. Although it would be tempting to interpret this finding in terms of insulin mediating the inhibitory effect of glucose on glucagon secretion, it should be noted that glucagon secretion is inhibited over a range of glucose concentrations with relatively small effects on insulin secretion. In fact, the stronger stimulation of insulin secretion occurring at glucose concentrations above 6 mmol/l coincides with stimulation (not inhibition) of glucagon secretion. Unlike what is seen in rat islets (33), Zn^{2+} stimulated glucagon secretion from human islets. The reason for this difference is unclear, but it is pertinent that several voltage-gated channels expressed in human α-cells are modulated by Zn^{2+} (A-currents, T-type Ca^{2+}-channels [34]). The stimulatory effects of insulin and Zn^{2+} may underlie the reduced inhibition of glucagon secretion seen above 6 mmol/l glucose (Fig. 1).

It has been proposed that glucose inhibits glucagon secretion by inhibition of K_{ATP}-channels, leading to membrane depolarization and voltage-dependent inactivation of voltage-gated ion channels involved in action potential firing (14). We have so far not observed consistent effects of glucose on membrane potential and conductance of isolated human α-cells. This may reflect technical difficul-

ties because electrical activity in these cells is very rarely stable enough to assess glucose effects, which develop over several minutes. However, tolbutamide promptly depolarized the α-cells by ~10 mV and decreased the peak voltage of the action potential, although it was without detectable effect on the resting membrane conductance. Thus, minute changes in K_{ATP}-channel activity have strong effects on α-cell electrical activity. Importantly, several of the voltage-gated membrane currents in human α-cells exhibit voltage-dependent inactivation, and this may account for the observed reduction of the action potentials peak voltage. Exocytosis in α-cells shows a strong dependence on voltage (Fig. 8*C*). A decrease in peak voltage of the action potential can therefore be expected to exert a strong inhibitory effect on glucagon secretion. A role of membrane depolarization mediated by closure of K_{ATP}-channels in the glucose-induced suppression of glucagon secretion is suggested by our previous finding that micromolar concentrations of the K_{ATP}-channel activator diazoxide antagonize the effect of the sugar (7).

The ion channel complements of human β- and α-cells show great similarities, and the inactivation and activation properties are very similar (20). Why then does membrane depolarization produced by tolbutamide stimulate insulin and somatostatin secretion (19,20) but inhibit glucagon secretion (7)? Key electrophysiological characteristics of human islet cells are summarized in supplementary Table 1, available in an online appendix. It can be seen that the α-cell differs from the other islet cells in having a low resting membrane conductance. Perhaps as a result of this, the interspike membrane potential of the α-cell is more depolarized than that of the β- and δ-cells. Another difference is that the Na^+-current, which contributes to the upstroke of the action potential, is smaller in the α-cells than in β- and δ-cells. The more depolarized interspike potential exacerbates this difference, and the Na^+-current that remains available for action potential firing is only ~1 pA/pF in α-cells compared with 12 pA/pF in β- and δ-cells.

In addition, α-cells can be distinguished from β-cells by the presence of a prominent A-type K^+-current. The functional significance of this current is underscored by the observation that heteropodatoxin-2, like the $K_V2.1/2.2$ antagonist stromatoxin, is a strong inhibitor of glucagon secretion. The transient hyperpolarization ("after-hyperpolarization," Fig. 7*A*) after each action potential that results from the activation of these channels may be particularly important for reactivation of the Na^+-channels in α-cells. Both types of K^+-currents undergo partial voltage-dependent inactivation at physiological membrane potentials, and the A-current is almost completely inactivated at the interspike potential attained in the presence of tolbutamide. It is possible that the β-cells have a greater capacity to repolarize the membrane voltage in the presence of tolbutamide (and glucose) because the downstroke of the action potential is due to opening of Ca^{2+}-activated BK-channels (20). These K^+-channels may be less susceptible to voltage-dependent inactivation, so that action potential height is maintained also during sustained membrane depolarization. More work is clearly needed to establish precisely how glucose regulates glucagon secretion. The findings reported here illustrate, however, that α-cell electrical activity depends on a complex balance between depolarizing and repolarizing conductances and that any process that perturbs this balance has dramatic effects on glucagon secretion.

ACKNOWLEDGMENTS

This work was supported by the MRC, the Wellcome Trust, and the NIHR. No potential conflicts of interest relevant to this article were reported.

R.R., C.W., M.S., J.N.W., S.A., and M.B. researched data, contributed to the discussion, and reviewed/edited the manuscript. P.R.J. contributed to the discussion and reviewed/edited the manuscript. P.R. and M.B. wrote the manuscript, contributed to the discussion, and reviewed/edited the manuscript.

We thank Dave Wiggins for excellent technical assistance.

REFERENCES

1. Cryer PE. Hypoglycaemia: the limiting factor in the glycaemic management of Type I and Type II diabetes. Diabetologia 2002;45:937–948
2. Lefebvre PJ (Ed.). Glucagon and Diabetes. In *Handbook of Experimental Pharmacology*. Berlin, Springer, 1996, p. 115–131
3. Gromada J, Franklin I, Wollheim CB. Alpha-cells of the endocrine pancreas: 35 years of research but the enigma remains. Endocr Rev 2007;28:84–116
4. Olofsson CS, Salehi A, Gopel SO, Holm C, Rorsman P. Palmitate stimulation of glucagon secretion in mouse pancreatic alpha-cells results from activation of L-type calcium channels and elevation of cytoplasmic calcium. Diabetes 2004;53:2836–2843
5. Gromada J, Bokvist K, Ding WG, Barg S, Buschard K, Renstrom E, Rorsman P. Adrenaline stimulates glucagon secretion in pancreatic A-cells by increasing the Ca2+ current and the number of granules close to the L-type Ca2+ channels. J Gen Physiol 1997;110:217–228
6. Miki T, Liss B, Minami K, Shiuchi T, Saraya A, Kashima Y, Horiuchi M, Ashcroft F, Minokoshi Y, Roeper J, Seino S. ATP-sensitive K+ channels in the hypothalamus are essential for the maintenance of glucose homeostasis. Nat Neurosci 2001;4:507–512
7. Macdonald PE, Marinis YZ, Ramracheya R, Salehi A, Ma X, Johnson PR, Cox R, Eliasson L, Rorsman P. A KATP Channel-Dependent Pathway within alpha Cells Regulates Glucagon Release from Both Rodent and Human Islets of Langerhans. PLoS Biol 2007;5:e143
8. Unger RH, Orci L. The role of glucagon in diabetes. Compr Ther 1982;8:53–59
9. Cryer PE. Glucagon and hyperglycemia in diabetes. Clin Sci 2008;114:589–590
10. Cryer PE, Davis SN, Shamoon H. Hypoglycemia in diabetes. Diabetes Care 2003;26:1902–1912
11. Bokvist K, Olsen HL, Hoy M, Gotfredsen CF, Holmes WF, Buschard K, Rorsman P, Gromada J. Characterisation of sulphonylurea and ATP-regulated K+ channels in rat pancreatic A-cells. Pflugers Arch 1999;438:428–436
12. Göpel SO, Kanno T, Barg S, Weng XG, Gromada J, Rorsman P. Regulation of glucagon release in mouse-cells by KATP channels and inactivation of TTX-sensitive Na+ channels. J Physiol 2000;528:509–520
13. Barg S, Galvanovskis J, Göpel SO, Rorsman P, Eliasson L. Tight coupling between electrical activity and exocytosis in mouse glucagon-secreting alpha-cells. Diabetes 2000;49:1500–1510
14. Rorsman P, Salehi SA, Abdulkader F, Braun M, Macdonald PE. K(ATP)-channels and glucose-regulated glucagon secretion. Trends Endocrinol Metab 2008;19:277–284
15. Brissova M, Fowler MJ, Nicholson WE, Chu A, Hirshberg B, Harlan DM, Powers AC. Assessment of human pancreatic islet architecture and composition by laser scanning confocal microscopy. J Histochem Cytochem 2005;53:1087–1097
16. Cabrera O, Berman DM, Kenyon NS, Ricordi C, Berggren PO, Caicedo A. The unique cytoarchitecture of human pancreatic islets has implications for islet cell function. Proc Natl Acad Sci U S A 2006;103:2334–2339
17. Lake SP, Bassett PD, Larkins A, Revell J, Walczak K, Chamberlain J, Rumford GM, London NJ, Veitch PS, Bell PR, et al. Large-scale purification of human islets utilizing discontinuous albumin gradient on IBM 2991 cell separator. Diabetes 1989; 38 (Suppl. 1):143–145
18. Ricordi C, Lacy PE, Finke EH, Olack BJ, Scharp DW. Automated method for isolation of human pancreatic islets. Diabetes 1988;37:413–420
19. Braun M, Ramracheya R, Amisten S, Bengtsson M, Moritoh Y, Zhang Q, Johnson PR, Rorsman P. Somatostatin release, electrical activity, membrane currents and exocytosis in human pancreatic delta cells. Diabetologia 2009;52:1566–1578
20. Braun M, Ramracheya R, Bengtsson M, Zhang Q, Karanauskaite J, Partridge C, Johnson PR, Rorsman P. Voltage-gated ion channels in human

pancreatic beta-cells: Electrophysiological characterization and role in insulin secretion. Diabetes 2008;57:1618–1628
21. Göpel SO, Kanno T, Barg S, Eliasson L, Galvanovskis J, Renstrom E, Rorsman P. Activation of Ca(2+)-dependent K(+) channels contributes to rhythmic firing of action potentials in mouse pancreatic beta cells. J Gen Physiol 1999;114:759–770
22. Zhang Q, Bengtsson M, Partridge C, Salehi A, Braun M, Cox R, Eliasson L, Johnson PR, Renstrom E, Schneider T, Berggren PO, Göpel S, Ashcroft FM, Rorsman P. R-type Ca(2+)-channel-evoked CICR regulates glucose-induced somatostatin secretion. Nat Cell Biol 2007;9:453–460
23. Salehi A, Vieira E, Gylfe E. Paradoxical stimulation of glucagon secretion by high glucose concentrations. Diabetes 2006;55:2318–2323
24. Marty A, Neher E. Potassium channels in cultured bovine adrenal chromaffin cells. J Physiol 1985;367:117–141
25. Conley E, Brammar W. VLH Kv4-Shal. In *The Ion Channel Facts Book: Voltage-gated Channels*. San Diego, CA, Academic Press, 1999, p. 617–646
26. Escoubas P, Diochot S, Celerier ML, Nakajima T, Lazdunski M. Novel tarantula toxins for subtypes of voltage-dependent potassium channels in the Kv2 and Kv4 subfamilies. Mol Pharmacol 2002;62:48–57
27. Zarayskiy VV, Balasubramanian G, Bondarenko VE, Morales MJ. Heteropoda toxin 2 is a gating modifier toxin specific for voltage-gated K+ channels of the Kv4 family. Toxicon 2005;45:431–442
28. Patel SP, Campbell DL. Transient outward potassium current, 'Ito', phenotypes in the mammalian left ventricle: underlying molecular, cellular and biophysical mechanisms. J Physiol 2005;569:7–39
29. Quoix N, Cheng-Xue R, Guiot Y, Herrera PL, Henquin JC, Gilon P. The GluCre-ROSA26EYFP mouse: a new model for easy identification of living pancreatic alpha-cells. FEBS Lett 2007;581:4235–4240
30. Singh V, Brendel MD, Zacharias S, Mergler S, Jahr H, Wiedenmann B, Bretzel RG, Plockinger U, Strowski MZ. Characterization of somatostatin receptor subtype-specific regulation of insulin and glucagon secretion: an in vitro study on isolated human pancreatic islets. J Clin Endocrinol Metab 2007;92:673–680
31. Banarer S, McGregor VP, Cryer PE. Intraislet hyperinsulinemia prevents the glucagon response to hypoglycemia despite an intact autonomic response. Diabetes 2002;51:958–965
32. Ravier MA, Rutter GA. Glucose or insulin, but not zinc ions, inhibit glucagon secretion from mouse pancreatic alpha-cells. Diabetes 2005;54:1789–1797
33. Franklin I, Gromada J, Gjinovci A, Theander S, Wollheim CB. Beta-cell secretory products activate alpha-cell ATP-dependent potassium channels to inhibit glucagon release. Diabetes 2005;54:1808–1815
34. Mathie A, Sutton GL, Clarke CE, Veale EL. Zinc and copper: pharmacological probes and endogenous modulators of neuronal excitability. Pharmacol Ther 2006;111:567–583